Pramana – J. Phys. (2018) 90:13
https://doi.org/10.1007/s12043-017-1502-0

Study of chaos in chaotic satellite systems

AYUB KHAN and SANJAY KUMAR*

Department of Mathematics, Faculty of Natural Sciences, Jamia Millia Islamia, New Delhi 110 025, India
*Corresponding author. E-mail: sanjay.jmi14@gmail.com

MS received 18 April 2017; revised 13 August 2017; accepted 18 August 2017;
published online 27 December 2017

Abstract. In this paper, we study the qualitative behaviour of satellite systems using bifurcation diagrams, Poincaré section, Lyapunov exponents, dissipation, equilibrium points, Kaplan–Yorke dimension etc. Bifurcation diagrams with respect to the known parameters of satellite systems are analysed. Poincaré sections with different sowing axes of the satellite are drawn. Eigenvalues of Jacobian matrices for the satellite system at different equilibrium points are calculated to justify the unstable regions. Lyapunov exponents are estimated. From these studies, chaos in satellite system has been established. Solution of equations of motion of the satellite system are drawn in the form of three-dimensional, two-dimensional and time series phase portraits. Phase portraits and time series display the chaotic nature of the considered system.

Keywords. Bifurcation diagram; Poincaré section map; Lyapunov exponents; perturbed satellite systems.

PACS Nos **05.45.Gg; 05.45.Tp; 05.45.Vx; 05.45.Pq**

1. Introduction

Satellite system is complex. Uncertainty and disturbances (external and internal disturbances) are parts of the satellite system. External disturbances may include aerodynamics moment, sunlight pressure torques, gravity gradient torque and magnetic moment, while internal disturbance includes parameters' uncertainties [1]. When disturbances occur in the drive satellite system, then controlling the relative error is directly associated with smaller errors than traditional tracking control [2,3].

The disturbances and uncertainty for satellite system occur in the form of chaos. It (chaos) is the state of disorder. It is the phenomenon of occurrence of bounded aperiodic evolution in completely deterministic nonlinear dynamical systems. Chaotic system is an inevitable phenomenon in nature. Organic evolution in nonlinear dynamical systems is highly sensitive to initial conditions. This sensitivity is popularly known as the butterfly effect [4–8]. The sensitivity to the initial conditions was first observed by Henri Poincaré (1913) and later by Lorenz (1963). Pioneer articles about chaotic systems were discussed by many researchers and authors (Sarkovski (1964), Smale (1967), Mandelbrot (1983), Devaney (1989), Stewart (1989) etc.).

Measure of chaos in the system is a tedious task. Tools such as bifurcation diagram, complexity, Poincaré section map, correlation dimension, Lyapunov exponents etc. are prerequisites for a good understanding of chaotic systems. Chaos in nonlinear systems can be observed by viewing bifurcations after varying the parameters of the chaotic system. Many researchers (Grassberger and Procaccia [9], Saha *et al* [10] and Litak *et al* [11]) have measured Lyapunov exponents in chaotic systems. Trajectories of Lyapunov exponents have been displayed through strange attractor which is framed of the complex patterns. The one of positive Lyapunov exponent value of a complex dynamical system is an indicator of chaos [10].

We need to pay much attention for the better understanding of satellite dynamics in space technology. The presence of satellites in orbits plays important roles in military, civil and scientific activities. A lot of work has been done in non-linear dynamics, such as chaotic attitude dynamics of satellite systems. Many researchers and scientists (Tsui and Jones [12]; Kuang and Tan [13]; Kuang *et al* [14]; Kong *et al* [15] etc.) have focussed on such studies. Controlling a Slave satellite is a synchronisation problem. For this, a reference trajectory for the Slave satellite depends on the states of the Master satellite system. In the formation of satellites applications, the objective will be to point the measuring instruments in the same direction. Therefore, let the reference trajectory of the Slave satellite be the measured attitude of the Master satellite [12,15].

In this paper, we present the basic concepts of bifurcation diagrams, Poincaré maps and Lyapunov exponents for dynamical systems. We formulate the chaotic satellite systems. We display the bifurcation diagrams of the satellite system with varying parameters. One-dimensional and two-dimensional Poincaré section maps of different phases of the satellite system are plotted. Lyapunov exponents and Kaplan–Yorke dimension are calculated. Dissipative nature of the satellite system is justified. We obtain equilibrium points of the chaotic satellite system and at each equilibrium point we obtain the eigenvalue of Jacobian matrix of the satellite system and verify the stability and instability region.

This paper is organised as follows: Section 1 gives introduction. Section 2 describes the basic concepts of bifurcation diagrams, Poincaré maps and Lyapunov exponents. In §3, we describe the satellite system. Numerical simulations are used to verify chaos in satellite system. Finally, conclusions are given in §4.

2. Some basic concept of bifurcation and Poincaré section phenomena

Bifurcation phenomena

Literally, bifurcation means splitting into two parts. Bifurcation occurs when a tiny smooth change is made to the parameter values of the dynamical system. Then sudden ‘qualitative’ or topological change in its behaviour is observed through the bifurcation diagram in the chaotic system. The point, where qualitative change in behaviour occurs, is known as the bifurcation point. The term ‘bifurcation’ was first coined by Henri Poincaré in 1885. It occurs in both continuous systems (described by ODEs, DDEs or PDEs) and discrete systems (described by maps) [10].

Poincare section phenomena

Poincaré map is one of the interesting tools to measure the qualitative behaviour of a dynamical system. It help to visualise the problems for both continuous as well as discrete dynamical systems. That is, it is a tool for presenting the trajectories of n-dimensional phase space into an $(n-1)$-dimensional space. After sowing one and more than one phase axes, an intersection surface is plotted. In continuous system, it is the intersection of periodic orbit in state space with lower dimensional subspace of given systems. A Poincaré map can be interpreted as a discrete dynamical system with a state space that is one dimension smaller than the original continuous dynamical system. It preserves many properties of periodic and quasiperiodic orbits of the original system and has a lower-dimensional state space. It is also used for analysing the original system in a simpler way [16]. It gives more informative snapshot of the flow than the full flow portrait of the system. When plotting the solutions to some nonlinear problems, the phase space can become overcrowded and the underlying structure may become obscured. To overcome these difficulties, Poincaré section map is used.

We consider the kth-dimensional system,

$$\dot{x} = f(x).$$

Let M be a $(k-1)$-dimensional surface of the section. This surface is transverse to the flow of the trajectories. The trajectories cross the surface and do not flow parallel to it. The Poincaré map is a mapping that goes from

$$M \to M,$$

this is obtained by taking every intersection from the trajectories one after the other. We shall denote x_n as the nth intersection and define the Poincaré map as

$$x_{n+1} = P(x_n).$$

Let $x_0 = f(x_0)$ be a fixed point in the map. The trajectory starting at this point comes back after some time T, and this is a closed orbit for the original system. The map P gets information about the stability of closed orbits near the fixed points.

Lyapunov exponents

One of the qualitative behaviour of the chaotic system is measured by Lyapunov exponents, named after the Russian Engineer Alexander M Lyapunov. A system have as many Lyapunov exponents as it has dimensions in its phase space. It is viewed that Lyapunov exponents are less than zero, indicating that all the nearby initial conditions converge on one another, and the initial small errors decrease with time. If one of the Lyapunov exponents is positive, then infinitesimally nearby initial conditions (points) diverge from one another exponentially fast. It means the errors in initial conditions will grow with time. This condition is known as sensitive dependence on initial conditions of chaos [10,16].

The quantitative test for the chaotic behaviour can sometimes distinguish it from noisy behaviour due to random, external influences. With the quantitative measure of the degree of chaoticity, we can see how chaos changes as the parameters are varied. Starting from two close initial values x_0 and y_0, we have

$$x_n = f(\kappa, x_{n-1}) = \cdots = f^n(\kappa, x_0)$$

and

$$y_n = f^n(\kappa, y_0),$$

where κ is a constant. If x_n and y_n are separated exponentially fast in the iterations, then

$$|y_n - x_n| = |y_0 - x_0|e^{nL} \quad (L > 0)$$

and

$$\frac{1}{n}\ln|y_n - x_n| \to L \quad \text{as} \quad n \to \infty.$$

This exponential separation phenomenon can occur if the two initial values are close enough to each other within a bounded region. Let

$$|y_0 - x_0| \to 0.$$

Before taking the limit $n \to \infty$, we define the constant as

$$\begin{aligned} L &= \lim_{n\to\infty} \frac{1}{n} \lim_{|y_0-x_0|\to 0} \ln\left|\frac{y_n - x_n}{y_0 - x_0}\right| \\ &= \lim_{n\to\infty} \frac{1}{n} \lim_{|y_0-x_0|\to 0} \ln\left|\frac{f^n(\kappa, y_0) - f^n(\kappa, x_0)}{y_0 - x_0}\right| \\ &= \lim_{n\to\infty} \frac{1}{n} \ln\left|\frac{\mathrm{d}f^n(\kappa, x_0)}{\mathrm{d}x_0}\right| \\ &= \lim_{n\to\infty} \frac{1}{n} \sum_{i=0}^{n-1} \ln\left|\frac{\mathrm{d}f^n(\kappa, x_i)}{\mathrm{d}x_i}\right| \end{aligned} \tag{1}$$

which is called the Lyapunov exponent of the trajectory

$$x_n = f^n(x_0), \quad n = 0, 1, \ldots.$$

Kaplan–Yorke dimensions

The Kaplan–Yorke dimension [9] of a chaotic system of order n is defined as

$$D_{\mathrm{KY}} = j + \frac{L_1 + L_2 + \cdots + L_j}{|L_{j+1}|}, \tag{2}$$

where $L_1 \geq L_2 \geq \cdots \geq L_n$ are the Lyapunov exponents of the chaotic system and j is the largest integer for which $L_1 + L_2 + \cdots + L_j \geq 0$. Kaplan–Yorke conjecture states that for typical chaotic systems, $D_{\mathrm{KY}} \approx D_L$, the information dimension of the system.

3. Numerical simulation

Attitude dynamics of the satellite in the inertial coordinate system [17–19] is written as

$$\dot{M} = T_a + T_b + T_c, \tag{3}$$

where M is the total momentum acting on the satellite. T_a, T_b and T_c are the flywheel torque, gravitational torque and disturbance torque respectively. The total momentum M is written as

$$M = Iw, \tag{4}$$

where I is the inertia matrix and w is the angular velocity.

The derivatives of the total momentum M is written as

$$\dot{M} = I\dot{w} + w \times Iw. \tag{5}$$

The symbol $\times$ stands for the cross-product of the vectors. Combining these equations, we get

$$I\dot{w} + w \times Iw = T_a + T_b + T_c. \tag{6}$$

We choose, $I = \mathrm{diag}(I_x, I_y, I_z)$

$$T_a = \begin{bmatrix} T_{ax} \\ T_{ay} \\ T_{az} \end{bmatrix}; \quad T_b = \begin{bmatrix} T_{bx} \\ T_{by} \\ T_{bz} \end{bmatrix}; \quad T_c = \begin{bmatrix} T_{cx} \\ T_{cy} \\ T_{cz} \end{bmatrix}.$$

The satellite system [2,17,18,20,21], is written as

$$\begin{aligned} I_x\dot{w}_x &= w_y w_z(I_y - I_z) + h_x + u_x, \\ I_y\dot{w}_y &= w_x w_z(I_z - I_x) + h_y + u_y, \\ I_z\dot{w}_z &= w_x w_y(I_x - I_y) + h_z + u_z, \end{aligned} \tag{7}$$

where u_x, u_y and u_z are the three control torques; and

$$\begin{aligned} h_x &= \left[(T_{ax} + T_{bx} + T_{cx})\right], \\ h_y &= \left[(T_{ay} + T_{by} + T_{cy})\right], \\ h_z &= \left[(T_{az} + T_{bz} + T_{cz})\right], \end{aligned}$$

where h_x, h_y and h_z are perturbing disturbance torques. We assume that $I_x > I_y > I_z = 1$. We take $I_x = 3$, $I_y = 2$ and $I_z = 1$. The perturbing torques [12] can be written as

$$\begin{pmatrix} h_x \\ h_y \\ h_z \end{pmatrix} = \begin{pmatrix} -1.2 & 0 & \sqrt{6}/2 \\ 0 & 0.35 & 0 \\ -\sqrt{6} & 0 & -0.4 \end{pmatrix} \begin{pmatrix} w_x \\ w_y \\ w_z \end{pmatrix}. \tag{8}$$

Three-dimensional chaotic satellite system is written as

$$\begin{aligned} \dot{x} &= \sigma_x yz - \frac{1.2}{I_x}x + \frac{\sqrt{6}}{2I_x}z, \\ \dot{y} &= \sigma_y xz + \frac{\sqrt{6}}{I_y}y, \\ \dot{z} &= \sigma_z xy - \frac{\sqrt{6}}{I_z}x + \frac{0.4}{I_z}z, \end{aligned} \tag{9}$$

where $\sigma_x = (I_y - I_z)/I_x$; $\sigma_y = (I_z - I_x)/I_y$; $\sigma_z = (I_x - I_y)/I_z$ and $\sigma_x = \frac{1}{3}$, $\sigma_y = -1$ and $\sigma_z = 1$.

Three-dimensional chaotic satellite system is rewritten as

$$\begin{aligned} \dot{x} &= (1/3)yz - ax + (1/\sqrt{6})z, \\ \dot{y} &= -xz + by, \\ \dot{z} &= xy - \sqrt{6}x - cz, \end{aligned} \tag{10}$$

where, a, b and c are known parameters. We have $a = 0.400$, $b = 0.175$ and $c = 0.400$.

3.1 *Lyapunov exponents and Kaplan–Yorke dimension*

Using the parameter values $a = 0.4$, $b = 0.175$ and $c = 0.4$, the Lyapunov exponents of satellite system (10) at $t = 300$ are obtained as: $L_1 = 0.1501$, $L_2 = 0.0050$ and $L_3 = -0.7802$. On calculating the Lyapunov exponents for 3D satellite system (10), we observe that out of these three Lyapunov exponents, one is positive, one is negative and one of these tends to zero which is the required condition for chaotic systems. It establishes that three-dimensional satellite system is chaotic. It is shown in figure 8. The maximal Lyapunov exponents of satellite system (10) is $L_1 = 0.1501$.

The sum of Lyapunov exponents are obtained as

$L_1 + L_2 + L_3 = -0.6251 < 0.$

Thus, it shows that satellite system (10) is dissipative. The Kaplan–Yorke dimension of satellite system (10) is obtained as

$$D_{\mathrm{KY}} = 2 + \frac{L_1 + L_2}{|L_3|} = 2.1988. \tag{11}$$

Figure 8 shows the dynamics of the Lyapunov exponents of satellite system (10).

3.2 *The system is dissipative*

In vector notation, we can rewrite system (10) as

$$\dot{X}(t) = f(x) = \begin{bmatrix} f_1(x, y, z) \\ f_2(x, y, z) \\ f_3(x, y, z) \end{bmatrix}, \tag{12}$$

where $X(t) = (x, y, z)$ and

$$f(x) = \begin{bmatrix} f_1(x, y, z) = (1/3)yz - ax + (1/\sqrt{6})z, \\ f_2(x, y, z) = -xz + by \\ f_3(x, y, z) = xy - \sqrt{6}x - cz \end{bmatrix},$$

where $a = 1.2$, $b = 0.175$ and $c = 0.4$.

We consider any region $\Lambda(t) \in R^3$ with a smooth boundary and $\Lambda(t) = \Theta_t(\Lambda)$, where Θ_t is the flow of f. Let $V(t)$ be the volume of $\Lambda(t)$. Using Liouville's theorem, we get

$$\dot{V}(t) = \int_{\Lambda(t)} (\nabla \cdot f)\mathrm{d}x\,\mathrm{d}y\,\mathrm{d}z. \tag{13}$$

The divergence of satellite system (10) is obtained as

$$\nabla \cdot f = \left[\frac{\partial f_1}{\partial x} + \frac{\partial f_2}{\partial y} + \frac{\partial f_3}{\partial z} = -a + b - c = -0.625\right]. \tag{14}$$

From (13) and (14), we obtain the first-order ordinary differential equation as

$$\dot{V}(t) = -0.625V(t). \tag{15}$$

Integrating eq. (15), we get the solution as

$$V(t) = \mathrm{e}^{-0.625t}V(0). \tag{16}$$

That is, the volumes of initial points are reduced by a factor of e with respect to time t. Thus, from eq. (16) $V(t) \to 0$ as $t \to 0$. The limit sets of the system is restricted to the specific limit set of zero volume. The asymptotic motion of satellite system (10) determines onto a strange attractor of the system. Thus, satellite system (10) has dissipative nature.

3.3 *Equilibrium points*

The equilibrium points of satellite system (10) are obtained by solving the following system of equations $\dot{X}(t) = 0$:

$$f(x) = \begin{bmatrix} (1/3)yz - ax + (1/\sqrt{6})z = 0 \\ -xz + by = 0 \\ xy - \sqrt{6}x - cz = 0 \end{bmatrix}.$$

Equilibrium points are

$$E_0 = \begin{bmatrix} 0 \\ 0 \\ 0 \end{bmatrix}, \quad E_1 = \begin{bmatrix} 1.1910 \\ 2.5766 \\ 0.3785 \end{bmatrix}, \quad E_2 = \begin{bmatrix} 0.1582 \\ -1.3641 \\ -1.5086 \end{bmatrix},$$
$$E_3 = \begin{bmatrix} -0.1582 \\ -1.3641 \\ 1.5086 \end{bmatrix}, \quad E_4 = \begin{bmatrix} -1.1910 \\ 2.5766 \\ -0.3785 \end{bmatrix}. \tag{17}$$

The Jacobian matrix of satellite system (10) is obtained by

$$J(X) = \begin{bmatrix} -a & 0.33 * z & (0.33 * y - 1/\sqrt{6}) \\ -z & b & -x \\ (y - \sqrt{6}) & x & -c \end{bmatrix}. \tag{18}$$

The Jacobian matrix at $E_0 = (0, 0, 0)$ is calculated as

$$J_0 = J(E_0) = \begin{bmatrix} -0.4 & 0 & 0.4082 \\ 0 & 0.175 & 0 \\ -2.4495 & 0 & -0.4 \end{bmatrix}. \tag{19}$$

In this equilibrium point, we obtain the eigenvalues, $\lambda_1 = -0.4 + 0.99\iota$, $\lambda_2 = -0.4 + 0.99\iota$ and $\lambda_3 = 0.175$. This equilibrium point E_0 is saddle-focus, which is unstable. The Jacobian matrix at $E_1 = (1.1910, 2.5766, 0.3785)$ is calculated as

$$J_1 = J(E_1) = \begin{bmatrix} -0.4000 & 0.1240 & 1.2585 \\ -0.3785 & 0.1750 & -1.1910 \\ 0.1271 & 1.1910 & -0.4000 \end{bmatrix}. \tag{20}$$

At this equilibrium point, we obtain the eigenvalues, $\lambda_1 = -0.7999$, $\lambda_2 = 0.0875 + 1.2075\iota$ and

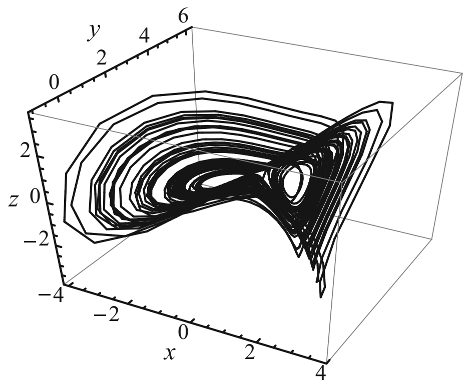

Figure 1. Three-dimensional phase portrait of the chaotic satellite system (without the controller).

$\lambda_3 = 0.0875 - 1.2075\iota$. This equilibrium point E_1 is saddle-focus, which is unstable. The Jacobian matrix at $E_2 = (0.1582, -1.3641, -1.5086)$ is calculated as

$$J_2 = J(E_2) = \begin{bmatrix} -0.4000 & -0.4978 & -0.0420 \\ 1.5086 & 0.1750 & -0.1582 \\ -3.8136 & 0.1582 & -0.4000 \end{bmatrix}. \tag{21}$$

At this equilibrium point, we obtain the eigenvalues, $\lambda_1 = 0.0875 + 0.8766\iota$, $\lambda_2 = 0.0875 - 0.8766\iota$ and $\lambda_3 = -0.8$. This equilibrium point E_2 is saddle-focus, which is unstable. The Jacobian matrix at $E_3 = (-0.1582, -1.3641, 1.5086)$ is calculated as

$$J_3 = J(E_3) = \begin{bmatrix} -0.4000 & 0.4978 & -0.0420 \\ -1.5086 & 0.1750 & 0.1582 \\ -3.8136 & -0.1582 & -0.4000 \end{bmatrix}. \tag{22}$$

At this equilibrium point, we obtain the eigenvalues, $\lambda_1 = 0.0875 + 0.8766\iota$, $\lambda_2 = 0.0875 - 0.8766\iota$ and $\lambda_3 = -0.8$. This equilibrium point E_3 is saddle-focus, which is unstable. The Jacobian matrix at $E_4 = (-1.1910, 2.5766, -0.3785)$ is calculated as

$$J_4 = J(E_4) = \begin{bmatrix} -0.4000 & -0.1240 & 1.2585 \\ -0.3785 & 0.1750 & 1.1910 \\ 0.1271 & -1.1910 & -0.4000 \end{bmatrix}. \tag{23}$$

At this equilibrium point, we obtain the eigenvalues, $\lambda_1 = -0.7999$, $\lambda_2 = 0.0875 + 1.2075\iota$ and $\lambda_3 = 0.0875 - 1.2075\iota$. This equilibrium point E_4 is saddle-focus, which is unstable. Thus, all these five equilibrium points of satellite system (10) are unstable equilibrium points.

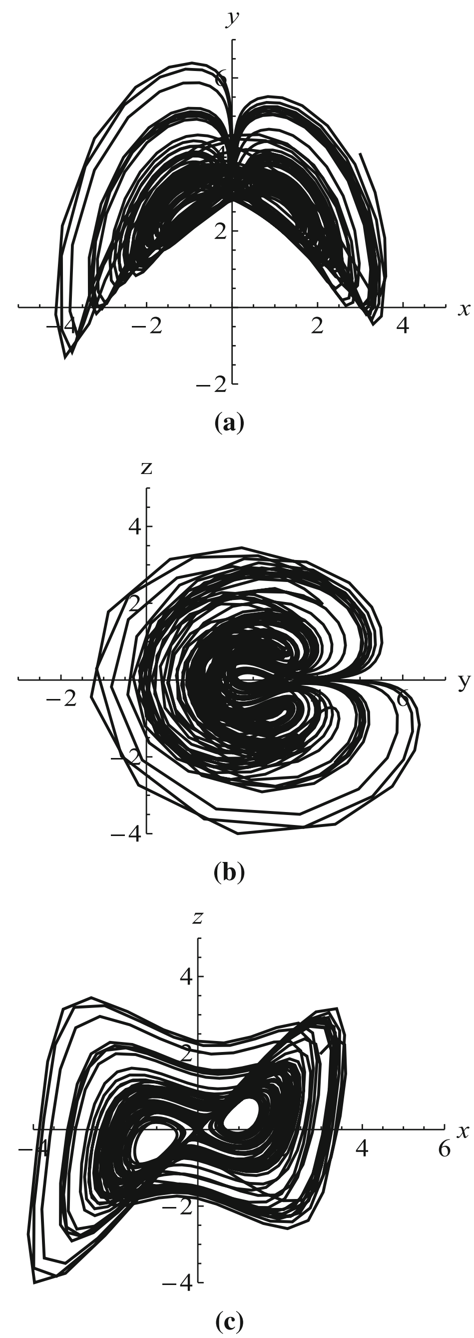

Figure 2. Two-dimensional phase portrait of the chaotic satellite system (without the controller).

3.4 *The y-axis is invariant*

From system equations (10), we observe that if $x(0) = 0$ and $z(0) = 0$, then x and z remain zero for all t. Thus the y-axis is an orbit, for which

$$\dot{y}(t) = by(t), \quad \text{hence } y(t) = y(0)\mathrm{e}^{bt}; \quad \text{for } x, z = 0. \tag{24}$$

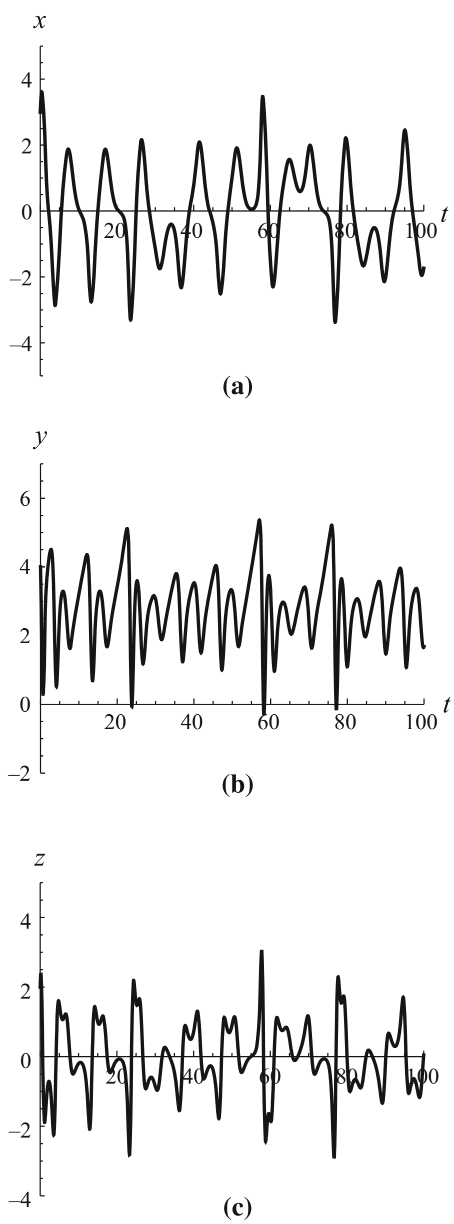

Figure 3. Time series graphs of the chaotic satellite system (without the controller).

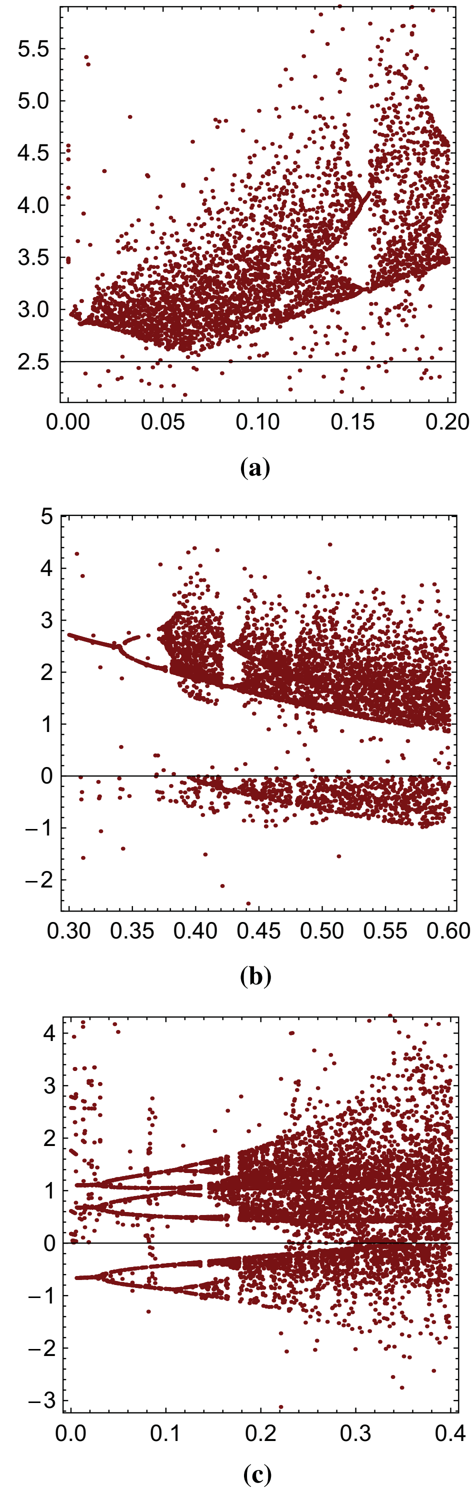

Figure 4. Bifurcation diagrams with the parameters a, b and c.

Thus the y-axis is part of the unstable manifold at the origin for the equilibrium.

Simulation

At initial condition for satellite systems $(x(0), y(0), z(0)) = (3, 4, 2)^T$, figure 1 shows the three-dimensional phase portrait of the chaotic satellite systems. Figures 2a–2c are shown as the two-dimensional phase portraits of the chaotic satellite system in the xy, yz and zx components with respect to time. Similarly, figures 3a–3c show time-series graphs of the satellite system. Figures 4a–4c show the bifurcation diagrams with respect to the parameters a, b and c respectively. Figures 5a–5c show the Poincaré section in one-dimensional phase portraits. We have sowed the axes x, y and z respectively. Different points for different orbits (sections) are shown using straight lines.

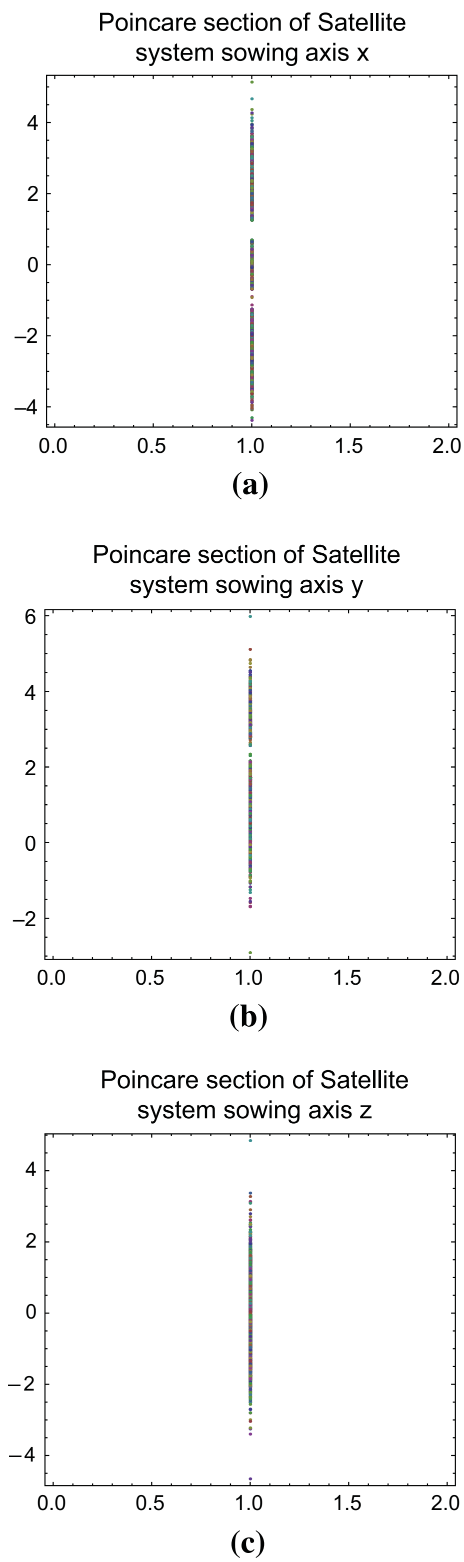

Figure 5. Poincaré section sowing the axes x, y and z.

Figures 6a–6c show the Poincaré section in two dimensions. We have sowed the axes xy, yz and zx and fixed $t = 0$–1, $t = 0$–3 and $t = 0$–3 respectively. We observe

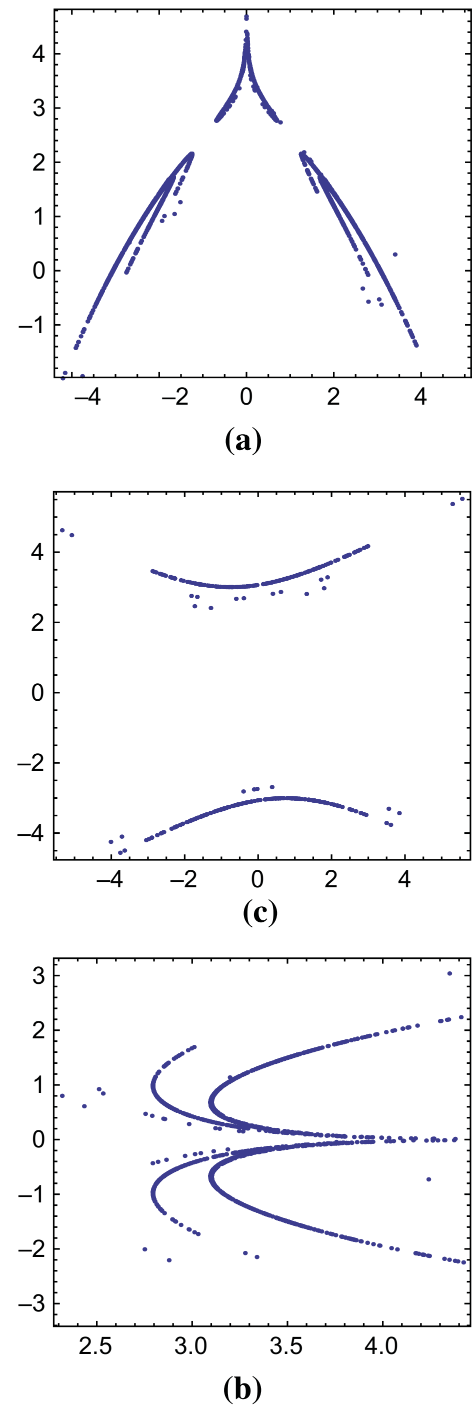

Figure 6. Poincaré section sowing the axes xy, yz and zx at (**a**) $t = 0$–1, (**b**) $t = 0$–3, (**c**) $t = 0$–3.

the strange attractor in these figures. Figures 7a–7c show the Poincaré section in two dimensions. We have sowed the axes xy, yz and zx at $z = 0$, $x = 0$ and $y = 0$ respectively. We find the strange attractor in these figures. We have computed the Lyapunov exponent of the satellite system, when $t = 300$. We have $L_1 = 0.1501$, $L_2 = 0.0050$ and $L_3 = 0.7802$. On calculating the Lyapunov exponents for the satellite system, we observe that

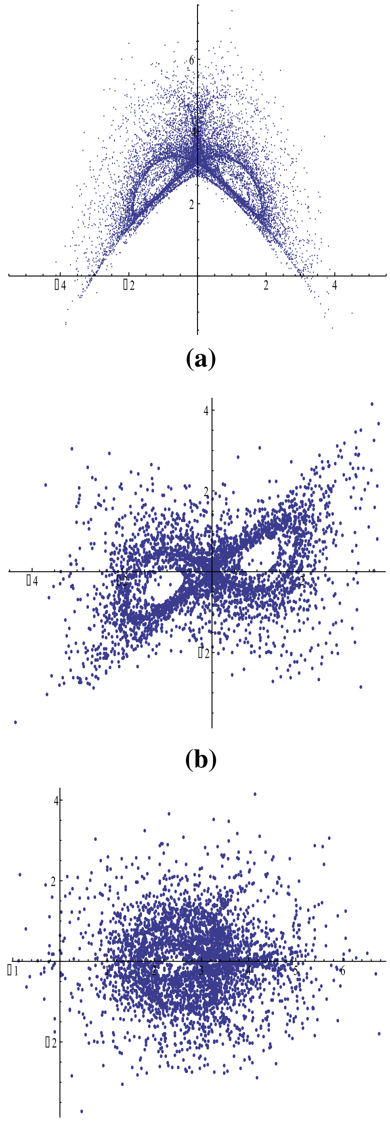

(a)

(b)

(c)

Figure 7. Poincaré section sowing the axes xy, yz and zx at (**a**) $z = 0$, (**b**) $x = 0$ and (**c**) $y = 0$.

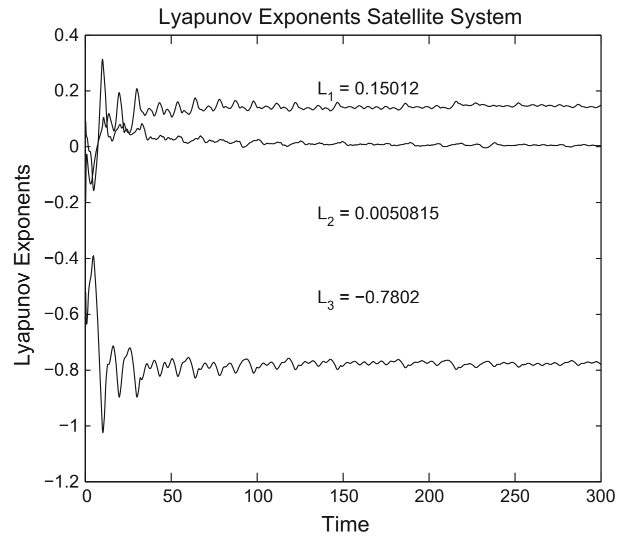

Figure 8. Lyapunov exponent of the chaotic satellite system.

out of these three Lyapunov exponent values, one is positive, one is negative and one of these tends to zero which is the required condition for a chaotic system indicating that satellite system is chaotic. It is shown in figure 8.

4. Conclusions

In this paper, we have measured chaos in the satellite system. We have used different tools such as the bifurcation diagrams, Poincaré section maps, dissipative as well as Lyapunov exponents and Kaplan–Yorke dimension for viewing chaos in the satellite system. We have observed that the qualitative behaviour of the satellite systems through bifurcation diagrams, Poincaré section maps and Lyapunov exponents confirm chaos in the satellite system. Bifurcation diagrams with respect to known parameters of the satellite systems have been analysed. Poincaré section with different sowing axes of the satellite are drawn. Lyapunov exponents are also calculated. These tools determine the existence of chaos. The Kaplan–Yorke dimension of the satellite system is $D_{\mathrm{KY}} = 2.1988$. Solution of the satellite system of equations are drawn in the form of three-dimensional, two-dimensional and time series phase portraits.

References

[1] G R Duan and H H Yu, *LMI in control systems analysis, design and applications* (CRC Press, Taylor and Francis Group, 2013)
[2] S Djaouida, *Int. J. Mech. Aerospace, Industrial, Mechatronic Manufacturing Eng.* **8**, 4 (2014)
[3] D Sadaoui *et al*, *Expert Syst. Appl.* **38**, 9041 (2011)
[4] A Khan and Shikha, https://doi.org/10.1007/s12043-017-1385-0, *Pramana – J. Phys.* (2017)
[5] A Khan, D Khattar and N Prajapati, https://doi.org/10.1007/s12043-016-1356-x, *Pramana – J. Phys.* (2017)
[6] A Khan and M A Bhat, https://doi.org/10.1007/s40435-016-0274-6, *Int. J. Dyn. Control* (2016)
[7] L M Pecora and T L Carroll, *Phys. Rev. Lett.* **64**, 821 (1990)
[8] T L Carroll and L M Pecora, *IEEE Trans. CAS I* **38**, 435 (1991)
[9] P Grassberger and I Procaccia, *Physica D* **9**, 189 (1983)
[10] L M Saha, M K Das and M Budhraja, *FORMA* **21**, 151 (2006)
[11] G Litak, A Syta, M Budhraja and L M Saha, *Chaos Solitons Fractals* **42**, 1511 (2009)

[12] A P M Tsui and A J Jones, *Physica D* **135**, 41 (2000)
[13] J Kuang and S H Tan, *J. Sound Vib.* **235(2)**, 175 (2000)
[14] J Kuang, S Tan, K Arichandran and A Y T Leung, *Int. J. Non-Linear Mech.* **36**, 1213 (2001).
[15] L Y Kong, F Q Zhoul and I Zou, The control of chaotic attitude motion of a perturbed spacecraft, in: *Proceedings of the 25th Chinese Control Conference*, Vol. 711 (Harbin, Heilongjiang, Augusth, 2006)
[16] Stephen Lynch, *Dynamical systems with applications using mathematica* (Birkhuser, Berlin, Boston, 2007)
[17] M J Sidi, *Spacecraft dynamics and control: A practical engineering approach* (Cambridge University Press, 1997)
[18] R W Zhang, *Satellite orbit and attitude dynamics and control* (in Chinese) (Beihang University Press, Beijing, China, 1998)
[19] T Liu and J Zhao, *Dynamics of spacecraft* (in Chinese) (Harbin Institute of Technology Press, Harbin, China, 2003)
[20] L L Show, J C Juang and Y W Jan, *IEEE Trans. Control Systems Technol.* **11(1)**, 73 (2003)
[21] W MacKunis, K Dupree, S Bhasin and W E Dixon, Adaptive neural network satellite attitude control in the presence of inertia and CMG actuator uncertainties, in: *American Control Conference* (Westin Seattle Hotel, Seattle, Washington, USA, June 11–13, 2008)